EFFECT OF ICE FORMATION ON AIRFOILS PERFORMANCE (PART-I)

Najdet N. Abdulla and Haitham Q. Hasoun

ABSTRACT

A numerical investigation was conducted to study the effect of simulated ice accreted on airfoil aerodynamics performance. The simulated ice shapes were tested on NACA 0012 airfoil wing at different Mach numbers. The study includes the one of the famous types of ice accreted on the airfoils called the rime ice.

The calculation of ice droplet trajectories was performed by solving the trajectories governing equations of the droplet using FVM. A numerical model based on staggered FVM is built up to solve the governing equations of a body fitted grid, trajectories equation, continuity equation and momentum equation using FORTRAN 97. The turbulence model of (k-ε) has been adopted in the programming to evaluate the turbulence effect. The program is valid for any type of 4 or 5 digits airfoil. The program is available to evaluate the rime ice accumulation. The pressure, lift, drag and pitching moment coefficients are computed and compared with that of clean case results. The program was run over different Mach numbers, to compare the results obtained at these Mach Numbers. The investigation of the work was tested on NACA 0012 in a range of angle of attack 0º to 6º, where stall starts at this angle of attack as demonstrated by the results.

The results show that the severity of ice formation could be more dangerous with increasing the angle of attack or the Mach number.

الخلاصة

أنجزت في هذا البحث الحسابات العددية لدراسة تأثير الثلج المقلد على أداء ديناميكيا الهواء المنساب على المطيار. أشكال الثلج المقلدة أختبرت على مطيار من نوع (NACA 0012) لأعداد ماخ مختلفة, وتضمنت الدراسة النوع المعروف من الثلج المتولد على سطح المطيار و هو الثلج الصقيع. لقد تم حساب مسار قطرة الثلج باعتماد المعادلة الحاكمة لمسارات قطرات الثلج وباستخدام طريقة الحجوم المحددة, و أعتمد الموديل الرياضي في ذلك طريقة (Staggered) لنظام الإحداثيات الغير المتعامدة في الشبكة المتولدة, ولمعادلة مسار القطرة, و معادلة الاستمرارية و معادلة الزخم باستخدام لغة البرمجة (فورتران 97) . تم استخدام الأنموذج الرياضي الأضطرابي (k-ε) لتحليل جريان المائع حول المطيار. ويمكن أستخدام البرنامج لأي نوع من أنواع (NACA airfoil) ذات ال 4 أو ال 5 أرقام وعلى بعدين فقط. البرنامج قادر على حساب تجمع تلك القطرات الثلجية المكونة للصقيع فوق المطيار والترويج. معاملات الضغط, قوة الرفع, قوة الكبح و عزم الترويج تم حسابها وقورنت مع حالة وجود الثلج على المطيار. أجريت الحسابات على أعداد ماخ ولزوايا مختلفة, وتم استخلاص النتائج وأخذت المقارنات للزوايا من (0º الى 6º) حيث يبدأ الانهواء بعد الزاوية (6º) كما بينت النتائج ذلك. أظهرت النتائج أن أشكال الثلج المتولد على المطيار تؤثر تأثيرا كبيرا على الأداء الديناميكي الهوائي وذلك بسبب تغير شكل الانسياب للمطيار مما يؤدي إلى زيادة معامل الكبح و نقصان معامل الرفع. كذلك أفادت النتائج بأن شدة الخطورة تكون أكثر حدة بزيادة عدد الماخ أو زيادة زاوية الهجوم.

INTRODUCTION

Icing on an airfoil or craft is defined as that condition where supercooled water droplets freeze on airframes or airfoil and form amount of ice which disturbs the airflow. In recent years, the number of icing related accidents has stimulated a renewed interest in the effect of icing on aerodynamic performance of aircraft (**Anderson, et al, 2001**). The formation of ice on aircraft components such as wings, control surfaces and engine intakes, occurs when the aircraft flies at a level where the temperature is at, or below freezing point and hits supercooled water droplets (**Anderson, et al, 2003**) and (**Anderson and Ching, 2003**).

The presence of ice accretion on unprotected aircraft components can lead to a number of aerodynamic penalties and consequently causes a serious safety problem. The most severe penalties encountered deal with decreased lift, increased drag, decreased stall angle, changes in the pressure distribution, vibration, early boundary layer separation, and reduced controllability. In fact, test data on ice effects indicate that the presence of ice on unprotected wing may increase drag by as much as 40% and reduce lift by 30% (**Bergrun, 1947**). To overcome these penalties, various practical methods have been used to remove or prevent accumulation of ice on aircraft surfaces by applying de-icing/anti-icing procedures. Modern types of airfoils have been developed, but, still needs specific ice protection systems to maintain their aerodynamic efficiency and safety margin.

Icing on aircraft occurs when the aircraft flies at a level where the temperature is at, or slightly below the freezing point and the atmosphere contains supercooled water droplets. When these droplets are hit by the aircraft they begin to freeze immediately. As the water droplets freeze, however, heat is released so that their temperature rises until 0ºC is reached. As this temperature is reached, freezing stops while the remaining liquid fraction of the droplets starts to run back along the surface of the aircraft or along existing ice and freeze downstream. The freezing fraction depends mainly on the temperature. At colder temperature a large part of a droplet freezes by impact while at higher temperature only a small part freezes while the remaining part freezes slowly (**Bragg, et al, 1982**).

The more dangerous types of ice are encountered in dense clouds, composed of heavy accumulations of large water droplets.

Icing is one of the most serious hazards for aircraft. Icing comes from the freezing of cloud droplets, or supercooled droplets which remain in liquid state even at temperatures far below freezing, when they are stuck by the aircraft during the flight. Cloud droplets may freeze instantaneously and form rime ice on unprotected surfaces or run downstream and freeze later forming glaze ice structure. Icing is most severe when temperature is near 0°C but may be encountered at temperature as low as -40 °C.

Icing is described as trace, light, moderate or severe which depends on the type of clouds, the type of aircraft, and the type of icing protection systems. The distribution of potential aircraft icing zones is mainly a function of cloud structure and temperature, which in turn vary with altitude, location and season. There are two types of clouds that may present icing conditions;

1) Stratiform clouds (continuous icing conditions) with horizontal extents up to 200 miles, altitudes 5,000 ft, liquid water content ranging from 0.1 g/m³ to 0.9 g/m³ and droplets diameter varying from 5 to 50 microns.

2) Cumuliform clouds (intermittent icing conditions) with vertical extents at altitude of 10,000 ft, horizontal extent of about 6 miles, liquid water content ranging from 0.1 g/m³ to 1.7 g/m³ and sometimes as high as 3.9 g/m³ or more, and droplets diameter similar to the case of stratiform clouds.

Icing can be serious when the cloud has high liquid water content. Some types of precipitation cause serious icing conditions while others may indicate the presence of serious icing in the vicinity. Freezing rain ahead of warm fronts presents a serious icing for aircraft flying near the top of the cold air mass beneath a deep layer of warm air. This is because rain drops are much larger than ordinary clouds droplets and may lead to high liquid water content. Icing may also comes from freezing drizzle just near the cloud base where the accretion on aircraft. Presently, more droplets are large.

Rime Ice Growth and Its Physics and Mechanism Process

The ice growth starts with the process of condensation. Water vapor condenses around particles and forms water droplet. The particles may grow up to 50μm or more. For larger droplets, such as rain drops which may exceed 1000μm, collision-coalescence and ice crystal theory must be included to explain growth process.

Rime ice is a dry, milky and opaque ice deposit which usually occurs at low airspeed, low temperature and low liquid water content. It is characterized by the instantaneous freezing of the incoming supercooled water droplets as soon as they hit the surface of the body trapping the air inside. As a consequence, the shape of the surface is altered generating performance penalties due to the loss in the aerodynamic characteristics and to the added weight which introduces an unbalance of the aircraft components during the flight, as shown in Fig. (1).

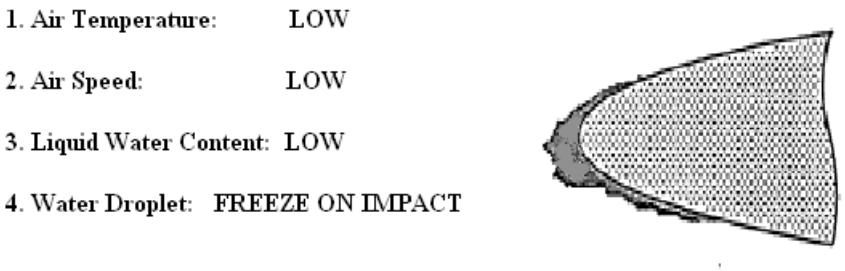

Fig. (1) Typical rime ice conditions on an airfoil [*Bergrun, N.R, 1995*].

The geometry of rime ice growth is shown below in Fig. (2);

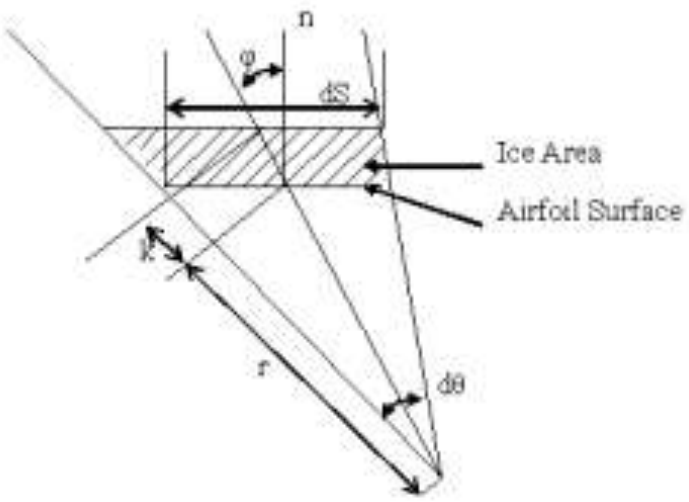

Fig. (2) Geometry of ice growth calculation [*Bragg M.B. and Kerho Michael, 1994*].

Important Factors and Parameters Affecting the Aircraft Icing

The amount and rate of icing depend on a number of meteorological and aerodynamic factors. Of primary importance are:

1- The amount of liquid water content of droplets.
2- The size of the liquid water droplets.
3- The temperature of aircraft surfaces.
4- The collection efficiency.
5- Icing intensity.
6- Air speed.

MATHEMATICAL FORMULATION

The main objective of ice simulation is the calculation of the impingement of the particles on the airfoil which determines the droplet impingement regions as well as the mass of liquid on the body surface.

The mathematical formulas are a process with a time-stepping procedure where successive thin ice layers are formed on the surface and followed by flow field and droplet impingement recalculations. The calculation of the water flux impinging on each grid forming the wing surface can be performed, then the ice accretion is calculated and the geometry is modified defining the ice shape for the first time step. The procedure is then performed for another time step to calculate a new ice layer.

Trajectory Calculations

To calculate the droplet trajectories, we assume that the volume of the droplet remains constant throughout the entire process. Although the droplet may or may not keep its spherical shape the droplet density ρ_d remains constant throughout the whole path, the initial droplet velocity is equal to

the free stream velocity U_∞ the droplets are much smaller than the body considered so that they do not affect the velocity field (**Bragg, 1988**).

The equation of motion of the droplet is given by (**Bragg and Kerho, 1994**);

$$a = \frac{1}{K}\left(\frac{C_D \,\mathrm{Re}}{24}\right)(u - v) \tag{1}$$

And K is the inertia parameter and define as;

$$K = \frac{\rho_d D_{eq}^2 U_\infty}{18 C\mu} \tag{2}$$

For Reynolds number below (1000) the following formula for Langmuir is used (**Langmuir and Blodgett, 1946**);

$$\frac{C_D \,\mathrm{Re}}{24} = 1 + 0.197\,\mathrm{Re}^{0.63} + 2.6 * 10^{-4}\,\mathrm{Re}^{1.38} \tag{3}$$

For Reynolds number higher than (1000) and below (3500) the formula (**Paraschivoiu and Brahimi, 1994);**

$$\frac{C_D \,\mathrm{Re}}{24} = 1.699 * 10^{-5}(\mathrm{Re}) \tag{4}$$

For Reynolds number higher than (3500) Hansoman formula's is used (**Hansoman, 1985**);

$$\frac{C_D \,\mathrm{Re}}{24} = 1.669 * 10^{-5}(\mathrm{Re})^{1.92} \tag{5}$$

Modified Inertia Parameter

The modified inertia parameter for (**Anderson and Ching, 2003**) formula is used in eq. (1) which is described as follows;

$$K_o = \frac{1}{8} + \frac{\lambda}{\lambda_{stokes}}\left(K - \frac{1}{8}\right) \tag{6}$$

Where

$$\frac{\lambda}{\lambda_{stokes}} = \left(0.8388 + 0.001483\,\mathrm{Re}_d + 0.1847\sqrt{\mathrm{Re}_d}\right)^{-1} \tag{7}$$

And

$$\mathrm{Re}_d = \frac{u(MVD)\rho_w}{\mu} \tag{8}$$

Turbulence Model (k-ε Model)

There are many two-equation models used in numerical today. Among them is the (k-ε) model. The reason of using the (k-ε) model is that in two-dimensional thin shear layers the changes in the flow direction are always so slow that the turbulence can adjust itself to local conditions, and if the convection and diffusion of turbulence properties can be neglected it is possible to express the influence of turbulence on the mean flow in terms of a simple model such the mixing length model, while if the convection and diffusion are not negligible (as in the case of flow around an airfoil) a compact algebraic prescription for the mixing length is no longer feasible, and the mixing length model lacks this kind of generality, so the way forward is to consider a statements regarding the dynamics of turbulence (**Versteeg and Malalasekera, 1995**).

In general form the transport equations for (k) and (ε) can be expressed in Cartesian coordinates as below (**Chung, 2002**):

$$\left(\rho u_j k\right)_{,j} = \left[\mu_k \left(k\right)_{,j}\right]_{,j} + \mu_t\left(\left(u_i\right)_{,j} + \left(u_j\right)_{,i}\right)\left(u\right)_{,j} + \frac{C_\mu \rho^2 k^2}{\mu_t} \tag{9}$$

$$\left(\rho u_j \varepsilon\right)_{,j} = \left[\mu_\varepsilon \left(\varepsilon\right)_{,j}\right]_{,j} + \frac{C_{\varepsilon 1}\varepsilon}{k}\mu_t\left(\left(u_i\right)_{,j} + \left(u_j\right)_{,i}\right)\left(u\right)_{,j} + \frac{C_{\varepsilon 2}\rho\varepsilon^2}{k} \tag{10}$$

Boundary Conditions and Properties

It is important to clear out the flying conditions and its properties, and these included the Mach number, pressure, ice density, ice intensity, air density, air viscosity, air temperature, LWC, droplet diameter, droplet effectiveness distance, and all these conditions are shown in table 3.1. Also the freezing fraction is taken 1.0, and the accretion time is taken in this work equal to 180 s. Table 1 below shows the properties and conditions of air and droplet.

Table 3.1 properties and conditions of air and droplet.

No.	Variable	Magnitude or quantity	Units
1	Mach number, M	0.3, 0.4 and 0.5	Nondimensional
2	Air pressure, P_a	101	kN/m²
3	Airfoil Chord	1	
4	Ice density, ρ_{ice}	1.2	g/cm³
5	Ice intensity	severe	non
6	Air density, ρ_a	1.2	kg/m³
7	Dynamic viscosity of Air	$17.1*10^{-6}$	N.s/m²
8	Altitude *h*	9000	m
9	Air temperature, T_a	-12.6	C°
10	LWC	1.0	g/m³
11	Droplet diameter	50	µm
12	Droplet effectiveness distance	4.5 of Chord length	Nondimensional

FLOW FIELD CALCULATION

The flow field calculation is needed to determine the velocity of air so that the droplet trajectory calculation can be solved. Where the equation of the airfoil that the flow field must flow over is;

$$y = \left(\frac{t}{0.2}\right) * \left(0.2969 * x^{0.5} - 0.126 * x - 0.3537 * x^2 + 0.2843 * x^3 - 0.1015 * x^4\right) \quad (11)$$

Where the basic equations governing incompressible and steady state fluid flow in Cartesian coordinates are the continuity and momentum equations stated as:

$$\left(u_i\right)_{,j} = 0 \quad (12)$$

$$\left(\rho u_j u_i\right)_{,j} = -P_{,i} + \left(\tau_{ij}\right)_{,j} \quad (13)$$

τ_{ij} is referring to the viscous stress tensor, and its constitutive relation in Newtonian fluid:

$$\tau_{ij} = \mu\left(\left(u_i\right)_{,j} + \left(u_j\right)_{,i}\right) - \frac{2}{3}\mu\frac{\partial u}{\partial x}.\delta_{ij} \quad (14)$$

The lift and drag equations governing the force over the airfoil are stated as:

$$C_L = \frac{2L}{\rho * V^2 * A} \tag{15}$$

$$C_D = \frac{2D}{\rho * V^2 * A} \tag{16}$$

Where the L and D is the summation of the components of the forces in the x- and y-direction:

$$L = F_y \cos(alpha) - F_x \sin(alpha) \tag{17}$$

$$D = F_x \cos(alpha) + F_y \sin(alpha) \tag{18}$$

GRID GENERATION

The O-grid type is selected to produce the grid generation using Poisson equations**.** The Elliptic grid generator is the most extensively developed method (**Hoffmann, 1989**), where it is commonly used for 2-D problems. A system of elliptic equations in the form of Poisson's equation is used, which is solved for the coordinates of the points in the physical domain:

$$\frac{\partial^2 \xi}{\partial x^2} + \frac{\partial^2 \xi}{\partial y^2} = P(\xi, \eta) \tag{15}$$

$$\frac{\partial^2 \eta}{\partial x^2} + \frac{\partial^2 \eta}{\partial y^2} = Q(\xi, \eta) \tag{16}$$

Fig. (3) shows the O-type grid generation using Poisson equation (PDE) with mesh of (71X37) at 0° angle of attack. Fig. (4) shows the O-type grid generation with mesh (151X71) at 6° angle of attack.

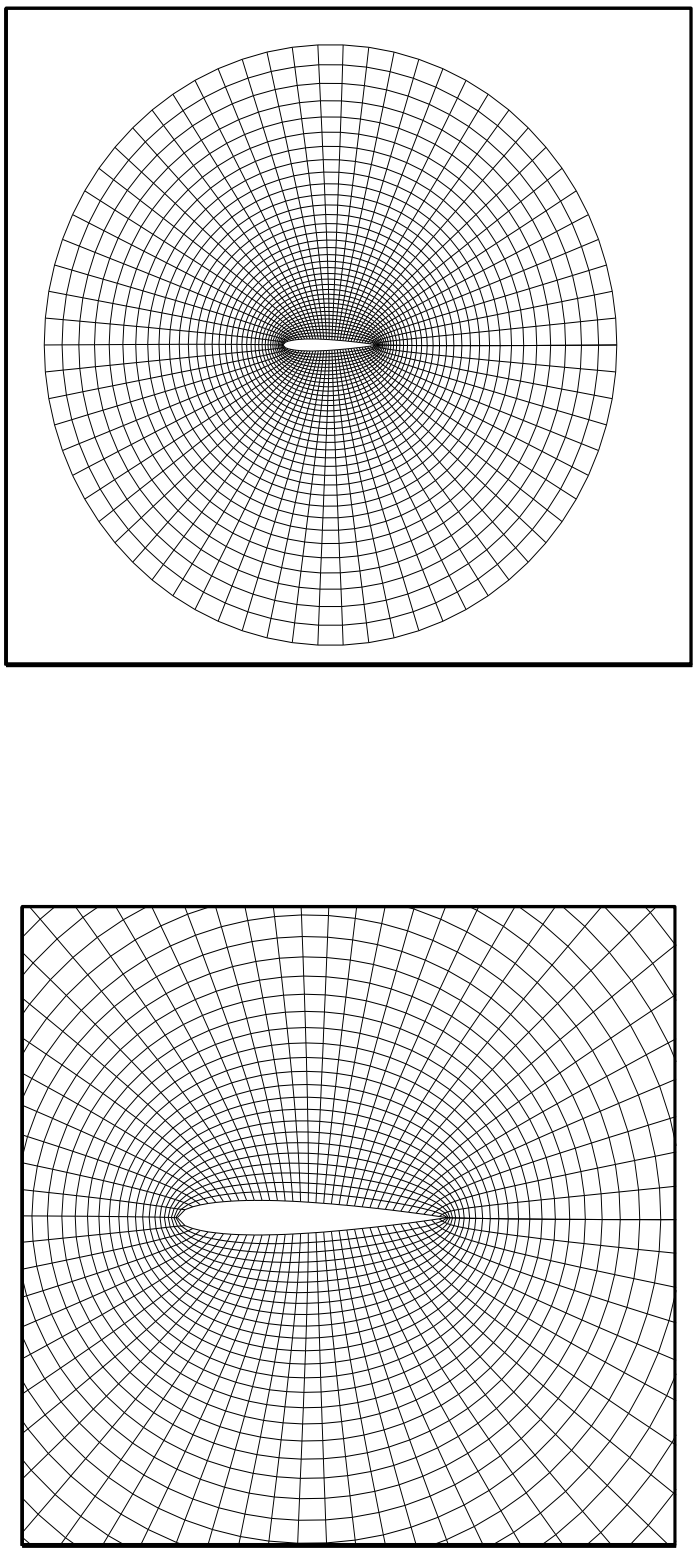

Fig. (3) PDE grid generation (O-type) of airfoil of mesh (71x37) with close view.

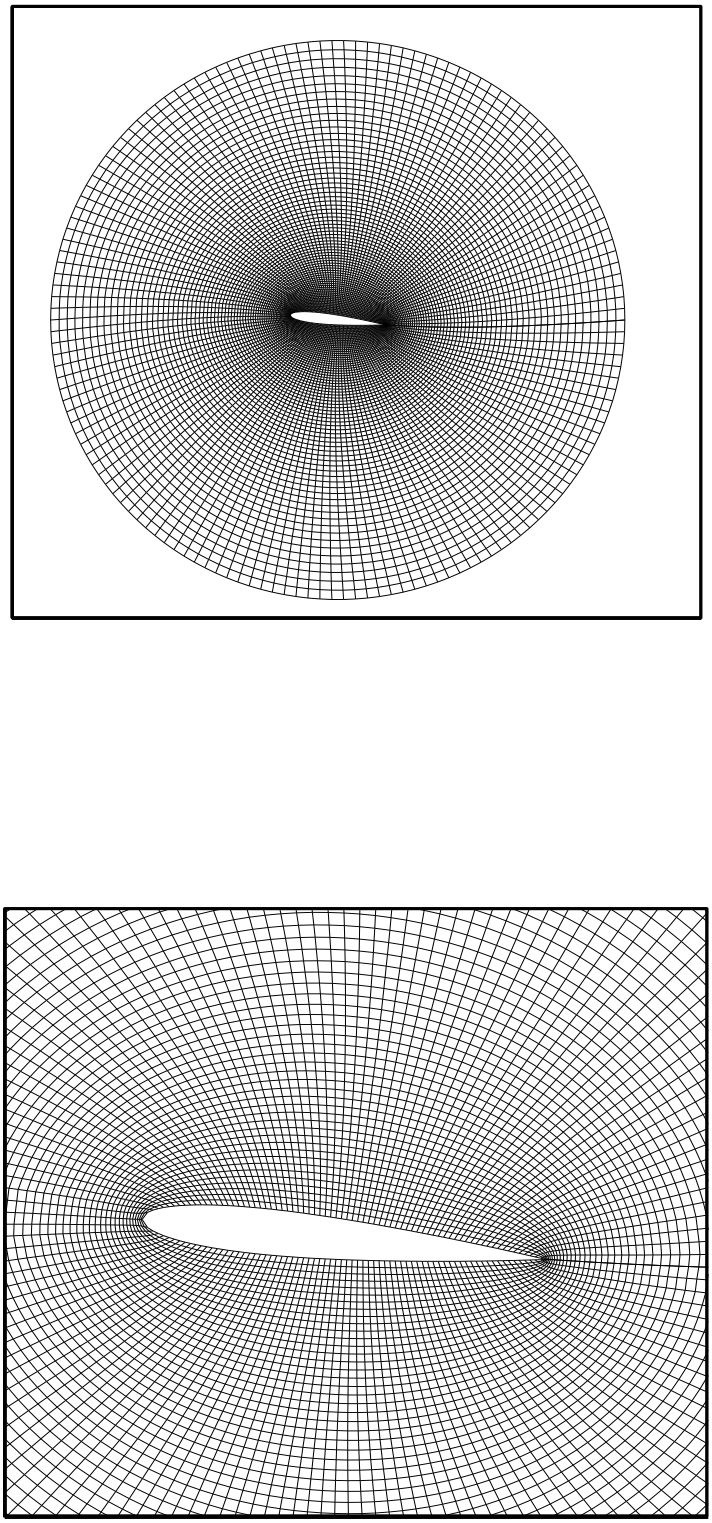

Fig. (4) PDE grid generation of airfoil at 6° angle of attack and mesh (151x71) with close view.

RESULTS

In clean case the results show that the increase in the angle of attack and Mach number cause a decrease in (C_P) on the upper surface of the airfoil, and increase the performance of the airfoil as shown in Figs. (5 through 7) at different Mach numbers (0.3, 0.4 and 0.5, respectively).

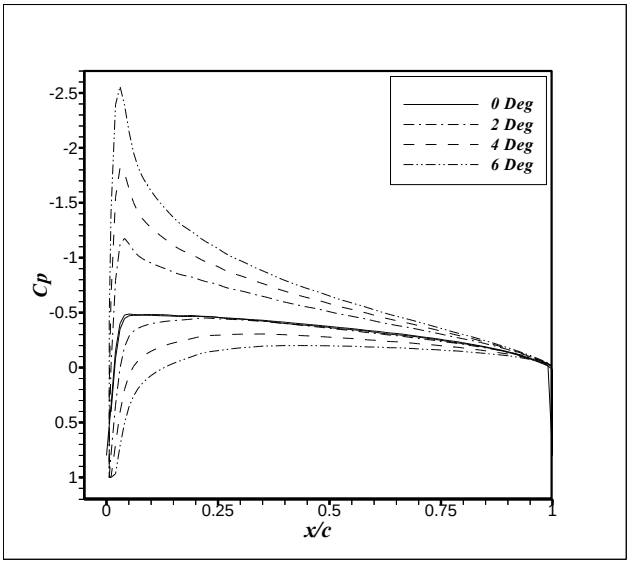

Fig. (5) Pressure coefficient distribution at M=0.3 for various angle of attack in clean case.

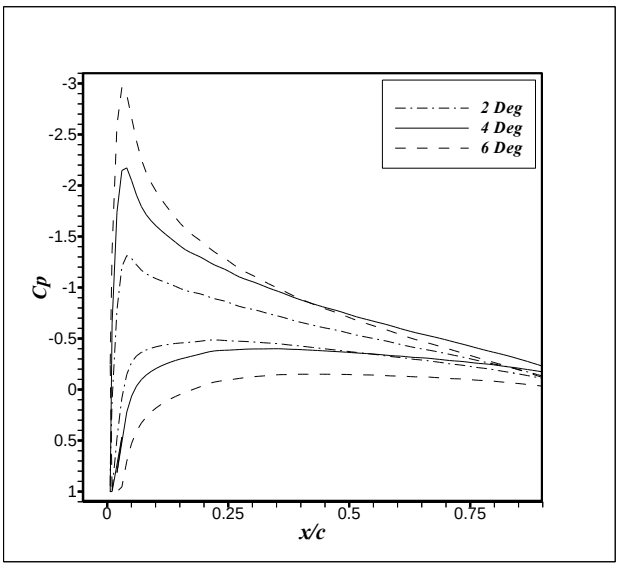

Fig. (6) Pressure coefficient distribution at M=0.4 for various angle of attack in clean case.

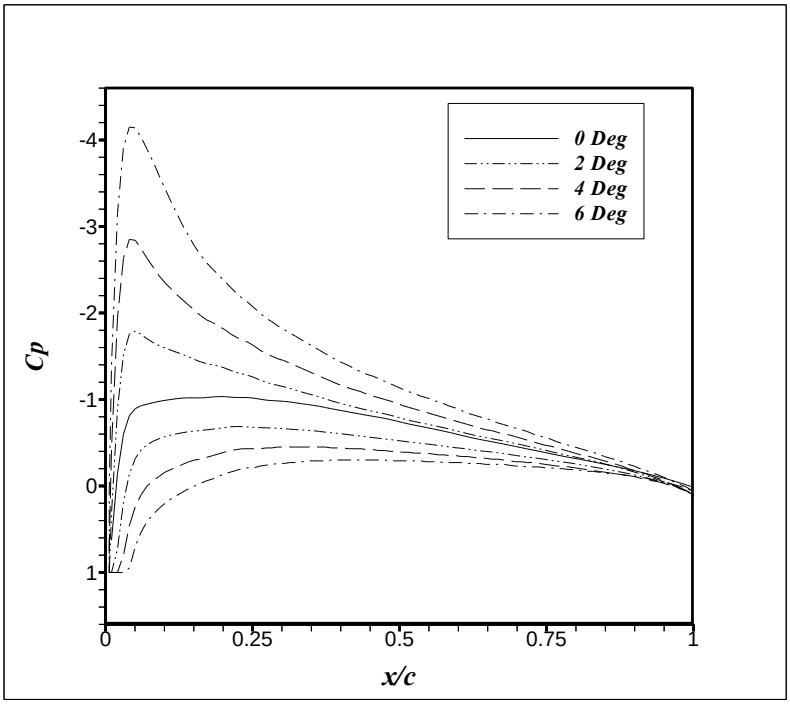

Fig. (7) Pressure coefficient distribution at M=0.5 for various angle of attack in clean case.

Figs. (8 through 11) show a comparison of (C_P) between the clean and rime ice case at different angle of attack and at constant M=0.3. The Figs. indicate that the increase in angle of attack would increase the (+ve) pressure coefficient in case of rime ice and hence decrease the airfoil performance. The ice formation at the nose of the airfoil caused a disturbance for the air flow over the airfoil and thereby cause uncouthly flow over the airfoil.

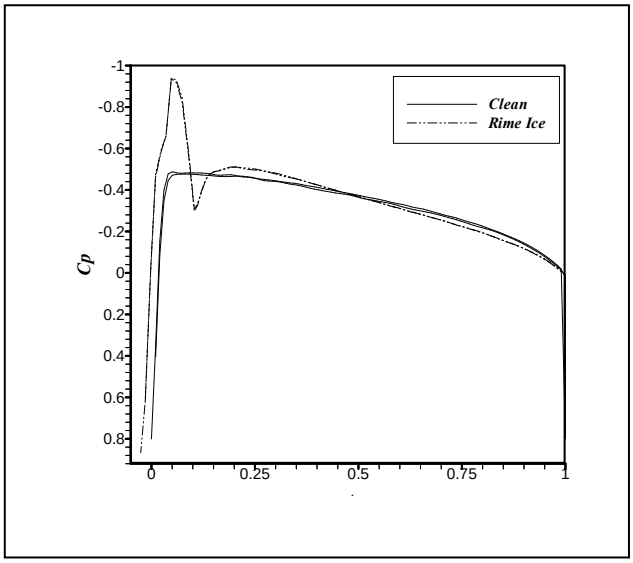

Fig. (8) Pressure coefficient distribution at (α=0°) and M=0.3 for clean and rime ice.

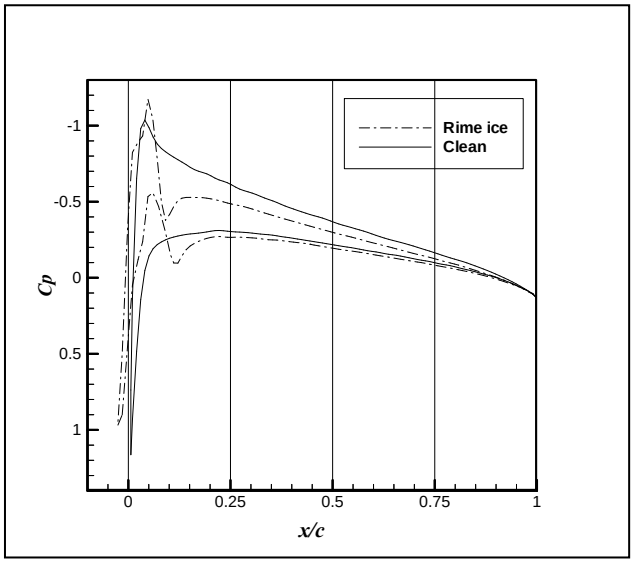

Fig. (9) Pressure coefficient distribution at (α=2°) and M=0.3 for clean and rime ice.

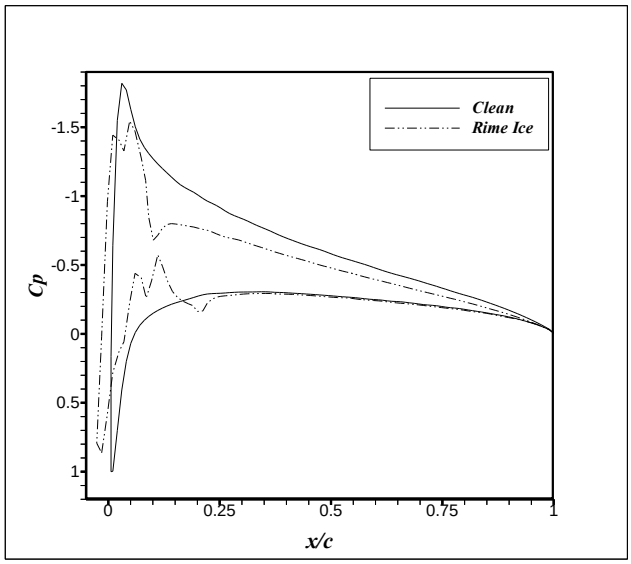

Fig. (10) Pressure coefficient distribution at (α=4°) and M=0.3 for clean and rime ice.

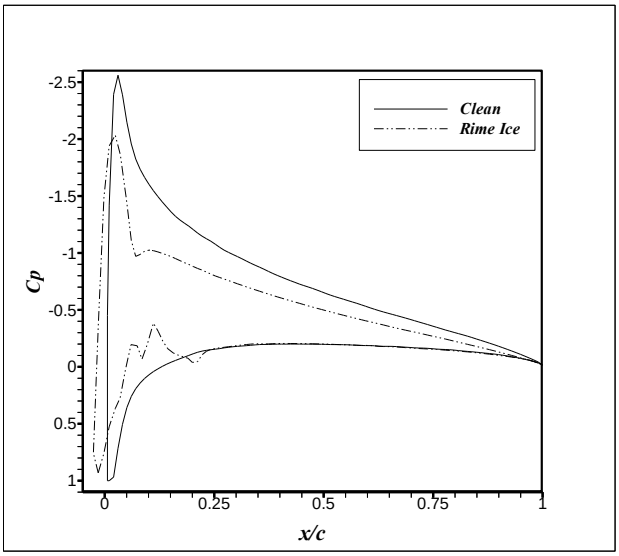

Fig. (11) Pressure coefficient distribution at (α=6°) and M=0.3 for clean and rime ice.

Figs. (12 through 15) show a comparison of (C_P) between the clean and rime ice case at different angle of attack and at constant M=0.4. Although the Figs. show that the increase in Mach number from 0..3 to 0.4 would decrease the pressure coefficient in case of rime ice, but in compassion to that in case of clean case the severity would be more dangerous than that at M=0.3. Where the difference between the clean case and that of rime ice case at M=0.3 is smaller that in case of M=0.4. Since the increase in the Mach number must lead to decrease pressure suction side, the Figs. above show that the increase in the angle of attack will not overcome the dangerous of the accreted ice on the airfoil. The performance will get worse due to the ice accretion, where the pitching moment will cause the airfoil to turn back with increasing the angle of attack which causes decrease in lift force so early.

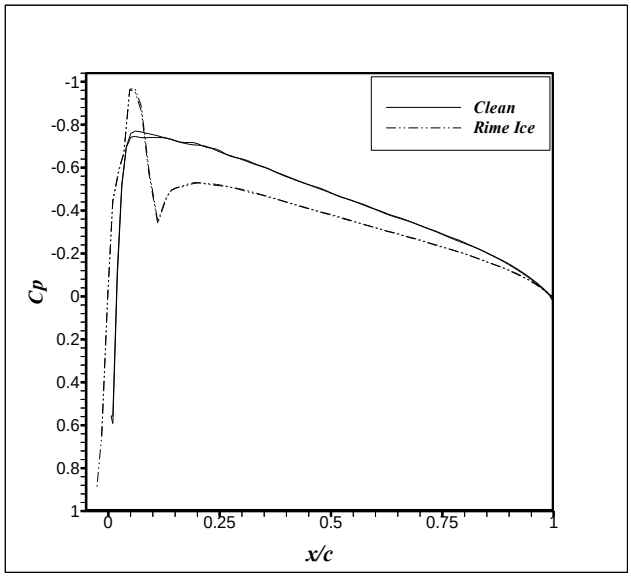

Fig. (12) Pressure coefficient distribution at (α=0°) and M=0.4 for clean and rime ice.

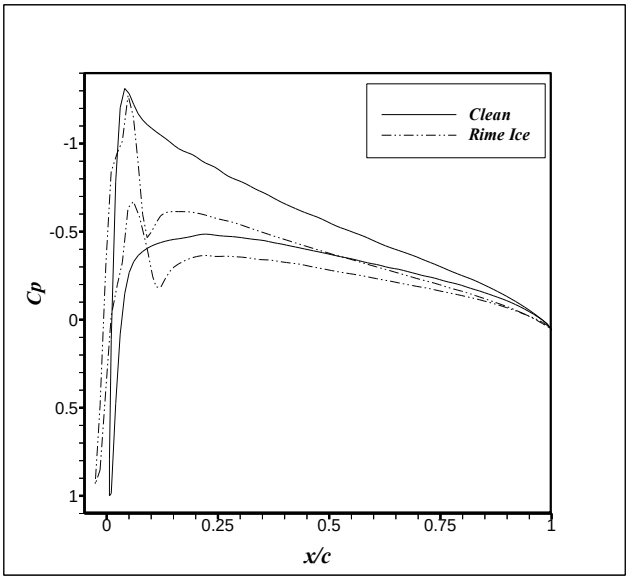

Fig. (13) Pressure coefficient distribution at (α=2°) and M=0.4 for clean and rime ice.

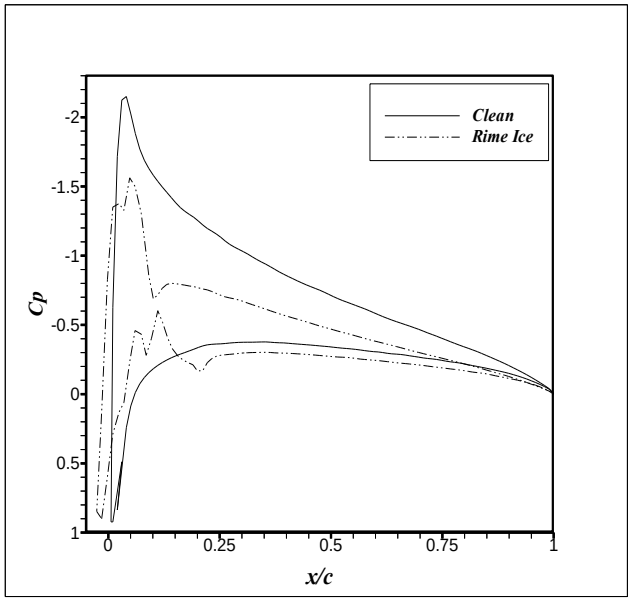

Fig. (14) Pressure coefficient distribution at (α=4°) and M=0.4 for clean and rime ice.

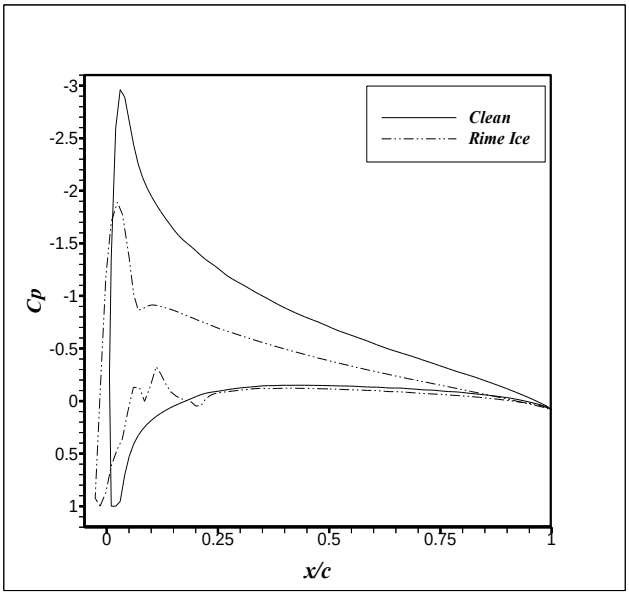

Fig. (15) Pressure coefficient distribution at (α=6°) and M=0.4 for clean and rime ice.

It is well known that any (nongeometrical) change in the airfoil shape would cause a decrease in the airfoil performance, and this can be figure out in lift and drag coefficients. Fig.(5.16) shows the decrease in lift coefficient if the rime ice accreted on the airfoil at M=0.3 when compared with the clean case. The Fig. shows that the difference in lift coefficient increases with increasing the angle of attack, while the value of C_L in the clean case increases to reach its maximum value ***0.68*** (at ***α=6°***). This value decreased from (***0.68***) to **(0.47)** at the same angle of attack when ice accreted. Also, C_L decrease from (***0.84***) to (***0.44***) for M=0.4 at the same angle of attack due to the existing of ice, where the ice disturb the smoothness flow of air over the airfoil, and from ***1.3*** to ***0.46*** for M=0.5 as shown in Figs.(5.17 and 5.18, respectively). Fig. (19) shows the lift coefficient deference is increased with increased the Mach number, which means that the increase in Mach number will not overcome the severity of the ice accumulation and will effect inversely.

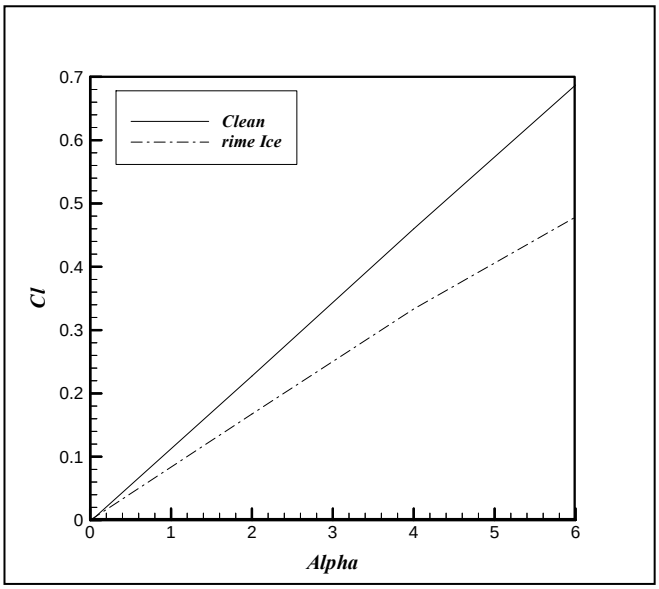

Fig. (16) Lift coefficient comparison between clean and rime ice at M=0.3.

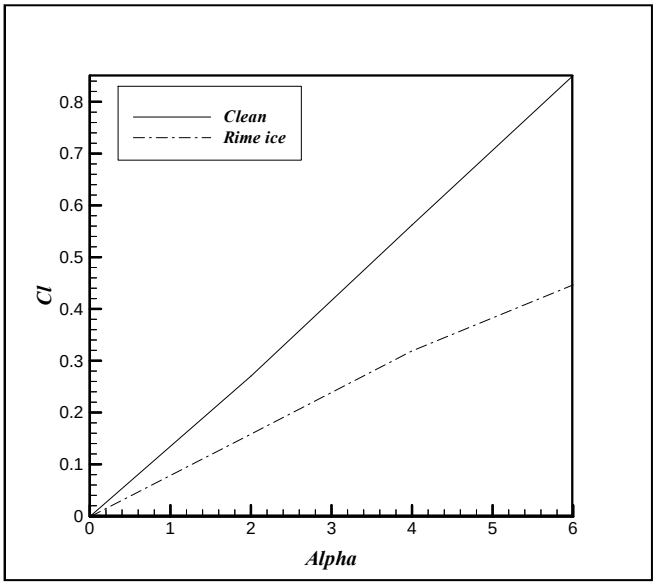

Fig. (17) Lift coefficient comparison between clean and rime ice at M=0.4.

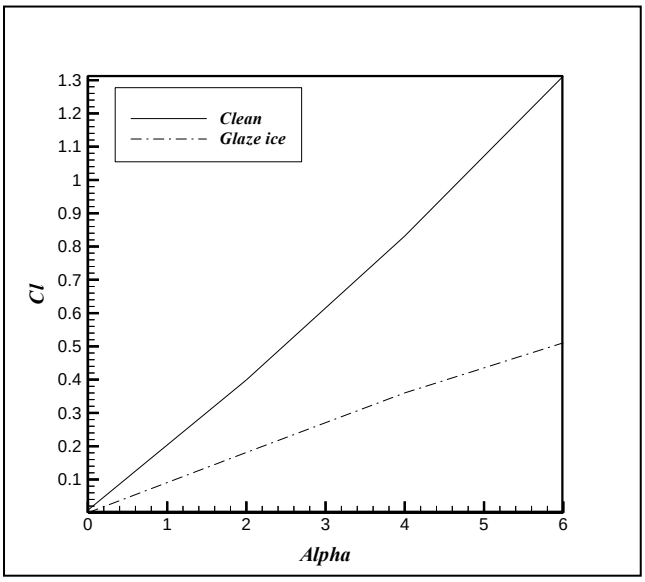

Fig. (18) Lift coefficient comparison between clean and rime ice at M=0.5.

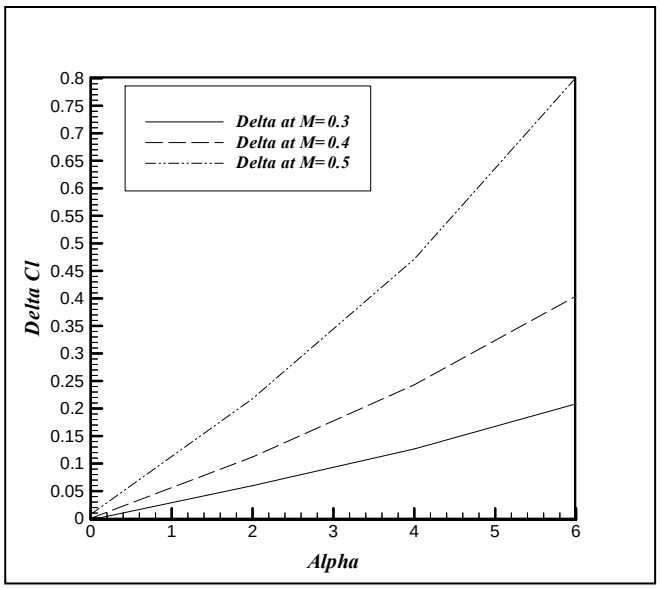

Fig. (19) Lift coefficient difference between clean and rime ice at deferent Mach numbers.

Fig. (20) shows the increase in drag coefficient due to the ice accretion compared with that of clean case, where the accreted ice cause more disturb for the air over the airfoil and thereby increase the drag force. Fig.(21) shows the increases in drag coefficient as Mach number increases along the angle of attack for the rime ice case, where the increase of velocity over the airfoil with ice accreted will lead to increase the disturbance of the flow, hence increase the drag coefficient. Fig.(22) shows the variation of (C_L) against (C_d) for rime case at different Mach number. The Fig. shows that the increase in Mach number would increase in the drag coefficient against the lift coefficient and this performance get wars as much as the Mach number increases.

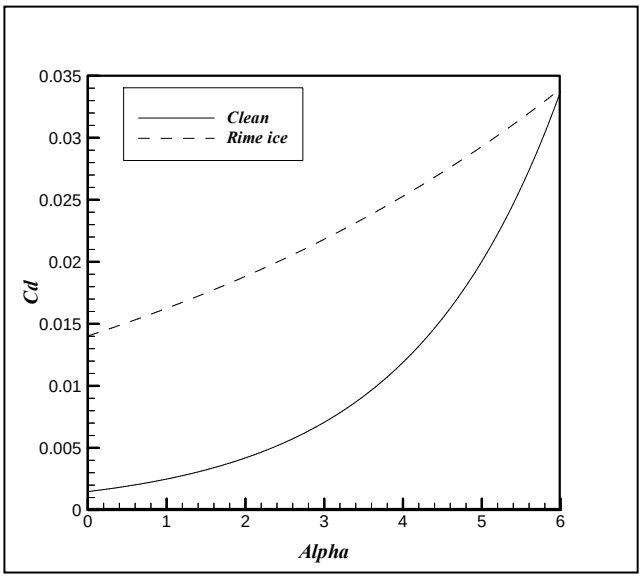

Fig. (20) Drag coefficient comparison between clean and rime ice at M=0.3.

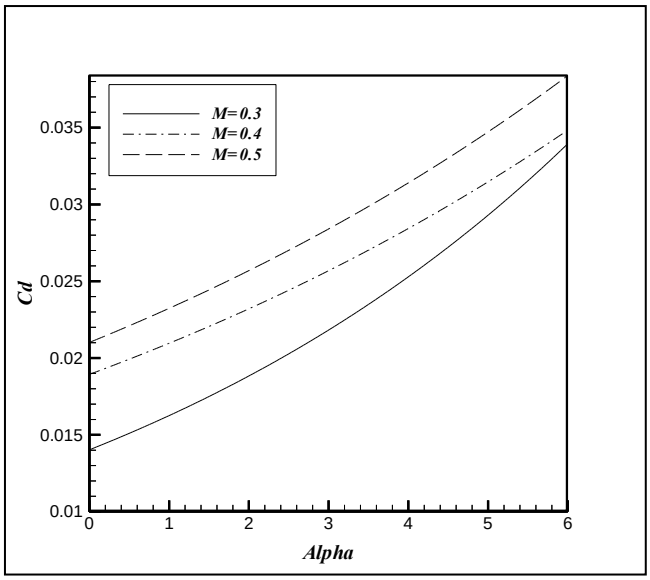

Fig. (21) Drag coefficient for rime ice at different Mach numbers.

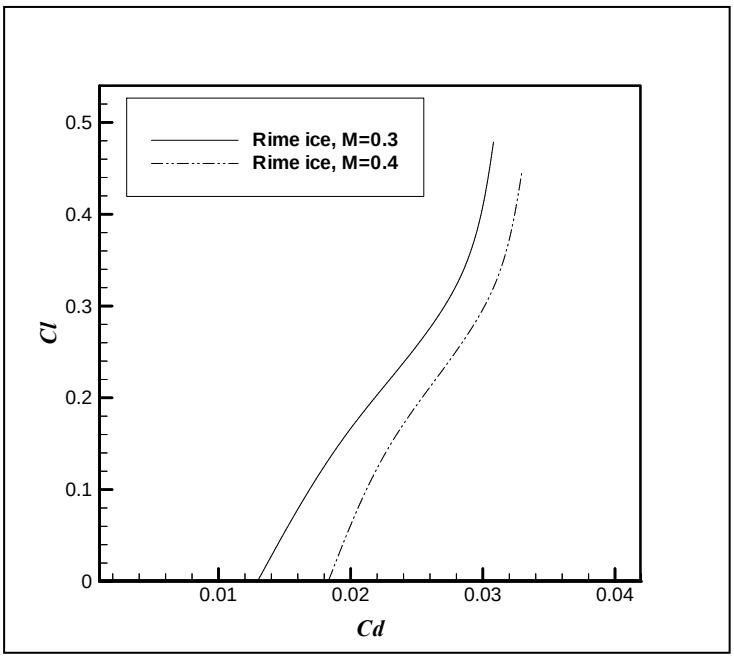

Fig. (22) Variation of C_L versus C_d for rime ice at different Mach numbers.

A comparison of a pitching moment coefficient versus angle of attack for the clean and rime ice case at Mach number (0.3) is shown in Fig.(23), it shows that the (C_m) in the iced case is higher than that in clean one, this gesticulate that the increase of instability when the shape of the airfoil is changed due to the ice accretion. This coefficient varies if the Mach number increases or decreases, especially in the ice case, while in the clean case the general behavior is the same. Fig.(24) shows the comparison at Mach number (0.4). More reliable comparison is made between the pitching moment coefficient and the lift force coefficient. This comparison shows the lift behavior versus the pitching moment as shown in Fig.(25) at M=0.3. It can be seen that the lift coefficient of the clean case is higher than that of the rime ice case and at the same time the pitching moment is higher for the ice case. Since the pitching moment is so high compare with that lifting force, the airfoil will be exposed to fall early in ice case. Fig. (26) shows the same comparison at M=0.4.

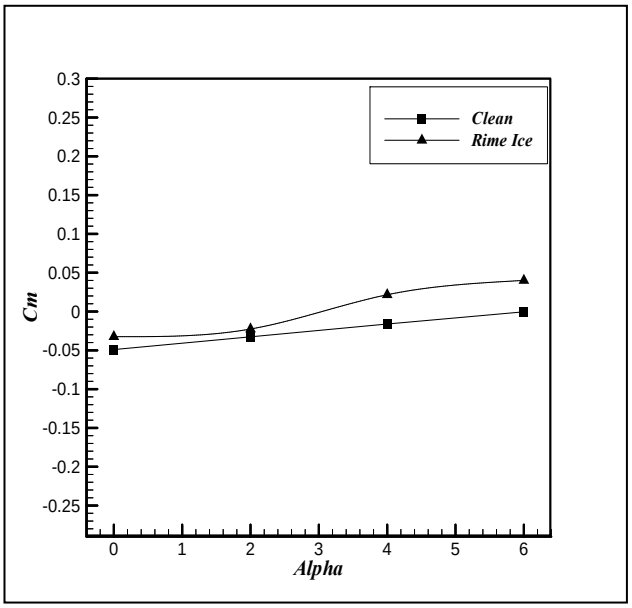

Fig. (23) Comparison pitching moment coefficient at M=0.3.

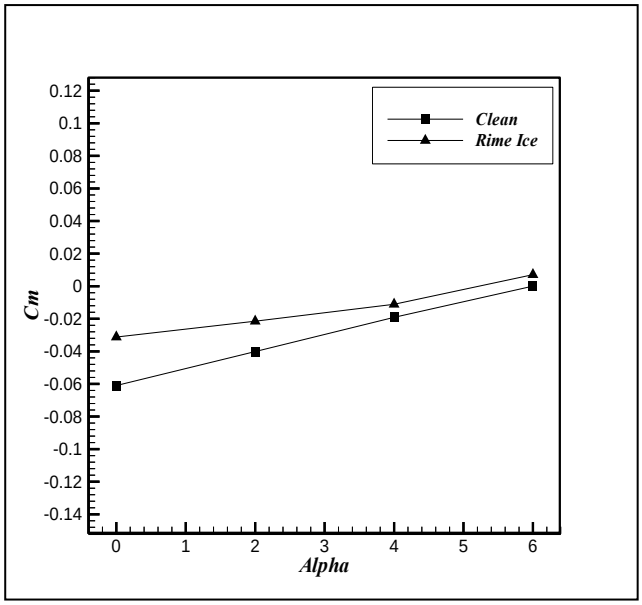

Fig. (24) Comparison pitching moment coefficient at M=0.4.

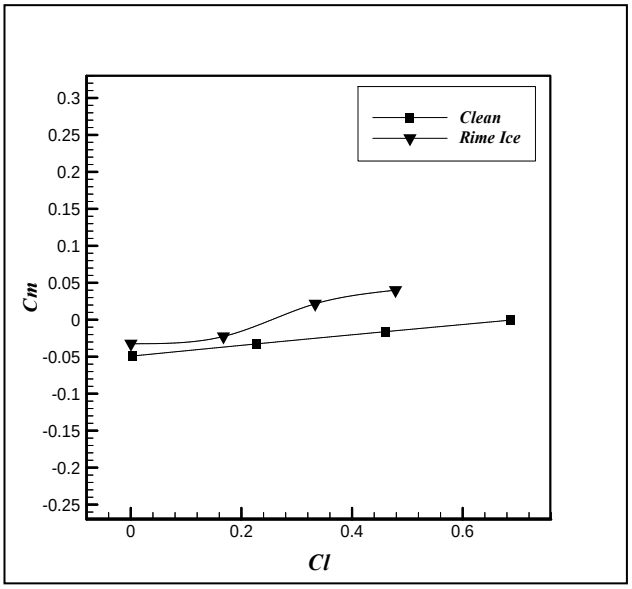

Fig. (25) Pitching moment coefficient versus lift coefficient at M=0.3.

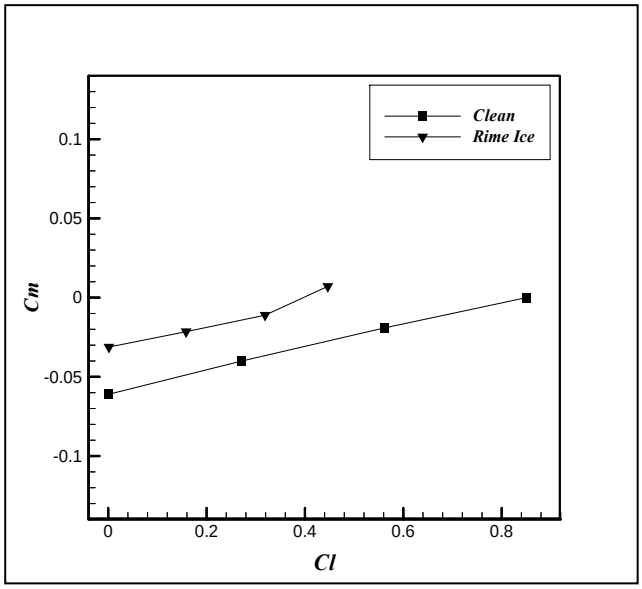

Fig. (26) Pitching moment coefficient versus lift coefficient at M=0.4.

Fig. (27) shows the effect of time accreted of ice at 6 time steps is considered, each of 30 second till reach the final steady state condition (180 s). Fig. (28) shows the distribution of pressure coefficient at that M=0.3 and α= 0°, where some one can see that the increase in time step (increase quantity of ice on the airfoil) will lead to increase the pressure coefficient, hence decrease the performance of the airfoil. Fig.(5.29) shows that the when the time step increased, the lift coefficient performance decreased. This is due to increase the disturbance of the air flow over the airfoil due to the ice. Fig.(30) shows the increase of the drag coefficient according to the increase and distortion in the airfoil nose area with increased of the ice accumulation.

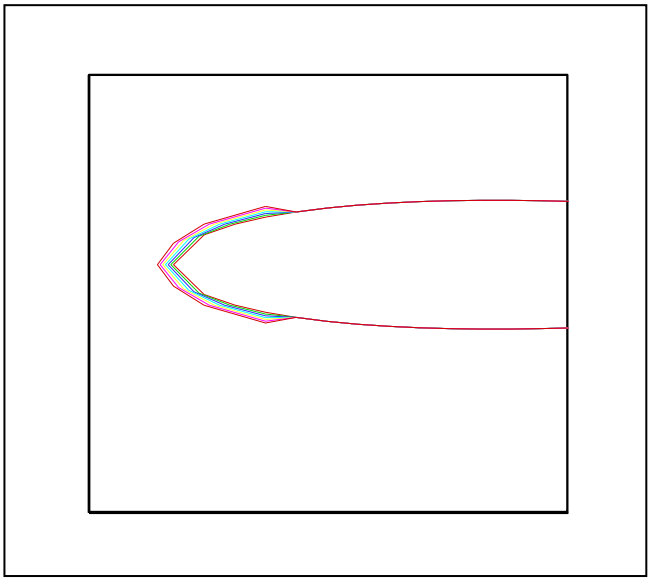

Fig. (27) Ice accreted on the airfoil of six time steps.

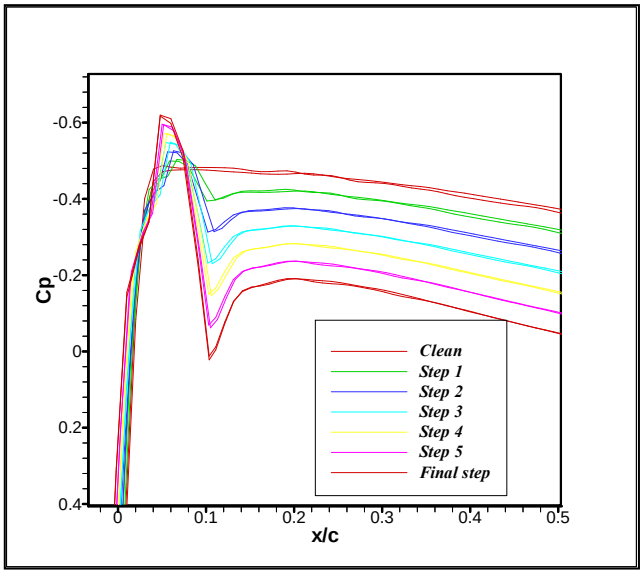

Fig. (28) Pressure coefficient distribution at M=0.3 and α=0° with different time step of ice accreted.

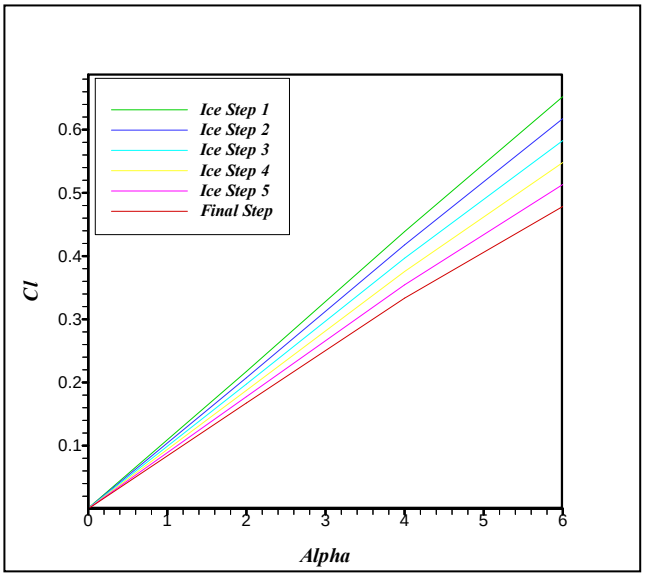

Fig. (29) Lift coefficient variation at M=0.3 and α=0° with different time step of ice accreted.

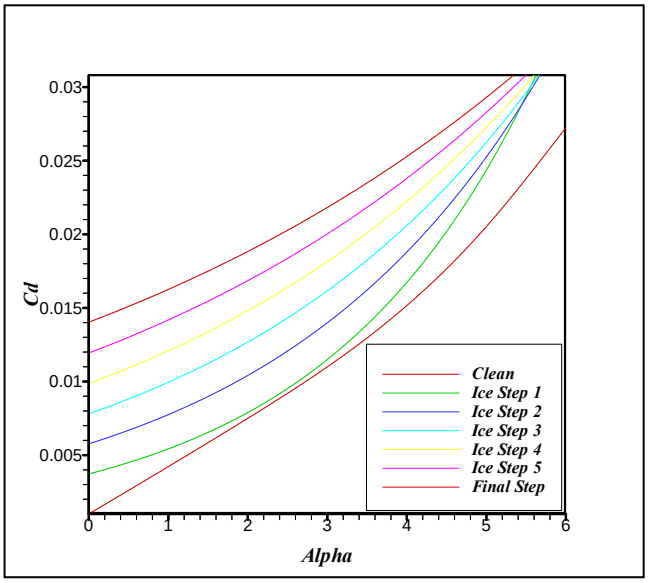

Fig. (30) Drag coefficient variation at M=0.3 and α=0° with different time step of ice accreted.

CONCLUSION

The icing on an airfoil was simulated with a renewed effect of time and collection efficiency and the airfoil performance showed severe aerodynamic penalties encountered with decrease in lift, and increase in drag and highly changes in the pressure distributions. The presence of ice on unprotected airfoil may increase drag by as much as 60% and reduce lift by 45%, where the severe adverse gradients will lower the C_l , as well as increasing the drag of the airfoil.

The drag and lift results for the ice cases show a severe deviation from that of the clean case, which indicate that the accretion ice on the airfoil is so dangerous and could cause big problems for the pilots.

The pitching moment coefficient increases in the case of ice accretion more than the clean case, where the average percentage increase of the pitching moment coefficient with the lift coefficient is 96 % and. This increase would cause an unstable condition for the flying condition.

NOMENCLATURES

a Acceleration of Ice Droplet (m/s²)

C Chord Length (m)

C_d Drag Coefficient

C_l Lift Coefficient

C_m Pitching Moment Coefficient

C_P Pressure Coefficient

D_d Droplet Diameter (μm)

D_{eq} Mean Volume Diameter (μm)

k Turbulent Kinetic Energy (m²/s²)

Re Reynolds Number

V Ice Droplet Velocity (m/s)

u Flow Field velocity (m/s)

U_∞ Free Stream Velocity (m/s)

K Inertia Parameter

Ko Modified Inertia parameter

μ Dynamic Viscosity (kg/m.s)

μ_k *Turbulent Dynamic Viscosity in k-Equation* (kg/m.s)

μ_ε *Turbulent Dynamic Viscosity in ε-Equation* (kg/m.s)

μ_t *Turbulent viscosity* (kg/m.s)

ρ_a *Air Density* (kg/m^3)

ρ_d *Ice Droplet Density* (kg/m^3)

ρ_w *Water Density* (kg/m^3)

(λ / λ_s) *Trajectory of a Droplet in Still Air to the Same Trajectory of the Droplet if the Drag is Assumed to Obey Stock's Law*

ξ , η *Curvilinear Coordinate Direction*

ε *Dissipation of Turbulent Kinetic Energy* (m^2/s^2)

σ_k *Empirical Constant in k Transport Equation*

σ_ε *Empirical Constant in ε Transport Equation*

REFERENCES

-Anderson David N., Galdemir C. Botura, Broeren Andy P., "A Study of Scaling For Intercycle Ice Accretion Tests", 39th Aerospace Sciences Meeting and Exhibit Reno, Nevada, Januarys- 11, 2001.

-Anderson David N., Hentschel Daniel B. and Ruff Gary A., "Measurement and Correlation of Ice Accretion Roughness". NASA/CR—2003-211823, AIAA–98–0486, June 2003.

-Anderson David N. and Tsao Jen-Ching, "Evaluation and Validation of the Messinger Freezing Fraction", Ohio Aerospace Institute, Brook Park, Ohio 44142. Prepared for the 41st Aerospace Sciences Meeting and Exhibit sponsored by the American Institute of Aeronautics and Astronautics Reno, Nevada, January 6–9, 2003.

-Bergrun, N.R., "A Method for Numerically Calculating the Area of Water Impingement on the Leading Edge of an Airfoil in a Cloud," NACA TN 1397, Aug. 1947.

-Bergrun, N.R., "Warming Trend for Icing Research," Aerospace America, pp. 22-27, Aug. 1995.

-Bragg M.B., Zaguli R.J., and Gregorek G.M. " Wind Tunnel Evaluation of Airfoil Performance Using Simulated Ice Shapes" Ohio State University Columbus, Ohio Prepared for Lewis Research Center Under Grant NAG3–28 NASA Contractor Report 167960, November 1982.

-Bragg, M.B., "Experimental Aerodynamic Characteristics of NACA 0012 Airfoil with Simulated Glaze Ice," AIAA Journal of Aircraft, Vol. 25, No. 9, pp. 849-854, Sept. 1988.

-Bragg M.B. and Kerho Michael F. "3-D Measurement on a 30-Degree Swept Wing with a Simulated Ice Accretion". University of Illinois, Urbana, IL, NACA Contact report, April 1994.

-Chung T. J. "Computational Fluid Dynamics", University of Alabama in Huntsville, Cambridge University Press, 2002.

-Hansoman R. john, "Droplet Size Distribution effects on aircraft ice accretion". J. Aircraft, vol. 22, No. 6, June 1985.

-Hoffmann Klaus A. "Computational Fluid Dynamics for Engineers", University of Texas at Austin, TX 78713-8148, USA, 1989.

-Langmuir, Irving, and Blodgett Katherine B.,"A Mathematical Investigation of Water Droplet Trajectories'" Army Air Process Technical Report No.5418 (Contract No. w-33-038-ac-9151), Feb. 1946.

-Paraschivoiu I., Tran P., and Brahimi M.T., "Prediction of Ice Accretion with Viscous Effects on Aircraft Wings," AIAA Journal of Aircraft, Vol. 31, No. 4, pp. 855-861, July-Aug. 1994, (also AIAA Paper 93-0027).

-Versteeg H. k. and Malalasekera W., "An Introduction to Computational Fluid Dynamics". Longman Group Ltd, 1995.